

Article

Determination of the Metabolite Content of *Brassica juncea* Cultivars Using Comprehensive Two-Dimensional Liquid Chromatography Coupled with a Photodiode Array and Mass Spectrometry Detection

Katia Arena ¹, Francesco Cacciola ^{2,*} , Laura Dugo ³, Paola Dugo ^{1,4} and Luigi Mondello ^{1,3,4,5}

¹ Department of Chemical, Biological, Pharmaceutical and Environmental Sciences, University of Messina, 98122 Messina, Italy; arenak@unime.it (K.A.); pdugo@unime.it (P.D.); lmondello@unime.it (L.M.)

² Department of Biomedical, Dental, Morphological and Functional Imaging Sciences, University of Messina, 98122 Messina, Italy

³ Department of Sciences and Technologies for Human and Environment, University Campus Bio-Medico of Rome, 00128 Rome, Italy; l.dugo@unicampus.it

⁴ Chromaleont s.r.l., c/o Department of Chemical, Biological, Pharmaceutical and Environmental Sciences, University of Messina, 98122 Messina, Italy

⁵ BeSep s.r.l., c/o Department of Chemical, Biological, Pharmaceutical and Environmental Sciences, University of Messina, 98122 Messina, Italy

* Correspondence: cacciola@unime.it; Tel.: +39-090-676-6570; Fax: +39-09-035-8220

Academic Editor: Patrick Chaimbault

Received: 14 February 2020; Accepted: 7 March 2020; Published: 9 March 2020



Abstract: Plant-based foods are characterized by significant amounts of bioactive molecules with desirable health benefits beyond basic nutrition. The Brassicaceae (Cruciferae) family consists of 350 genera; among them, *Brassica* is the most important one, which includes some crops and species of great worldwide economic importance. In this work, the metabolite content of three different cultivars of *Brassica juncea*, namely ISCI Top, “Broad-leaf,” and ISCI 99, was determined using comprehensive two-dimensional liquid chromatography coupled with a photodiode array and mass spectrometry detection. The analyses were carried out under reversed-phase conditions in both dimensions, using a combination of a 250-mm microbore cyano column and a 50-mm RP-Amide column in the first and second dimension (²D), respectively. A multi (three-step) segmented-in-fraction gradient for the ²D separation was advantageously investigated here for the first time, leading to the identification of 37 metabolites. In terms of resolving power, orthogonality values ranged from 62% to 69%, whereas the corrected peak capacity values were the highest for *B. juncea* ISCI Top (639), followed by *B. juncea* “Broad-leaf” (502). Regarding quantification, *B. juncea* cv. “Broad-leaf” presented the highest flavonoid content (1962.61 mg/kg) followed by *B. juncea* cv. ISCI Top (1002.03 mg/kg) and *B. juncea* cv. ISCI 99 (211.37 mg/kg).

Keywords: *Brassica juncea* spp.; metabolites; foods; comprehensive two-dimensional liquid chromatography; mass spectrometry; multi segmented-in-fraction gradient

1. Introduction

Vegetables from the Brassicaceae or Cruciferae family represent the most commonly consumed vegetables worldwide. This family includes brussels sprouts, broccoli, cabbage, cauliflower, and others. Such vegetables do contain high levels of bioactive compounds, e.g., polyphenols, carotenoids, tocopherols, glucosinolates, and ascorbic acid [1–4]. Epidemiological data have demonstrated the

ability of *Brassica* vegetables to decrease the risk of cardiovascular diseases and several types of cancer, e.g., such as in the gastrointestinal tract [5]. All these effects have been associated with the presence of bioactive molecules with antioxidant and free radical scavenging properties, with potential effects on gene expression, cell signaling, and cell adhesion [6].

Among the bioactive compounds that occur in the Brassicaceae family, polyphenols represent a group of secondary plant metabolites comprising diverse families [7]. Among them, the most common subclass of polyphenols is represented by flavanols, and the most abundant aglycones are quercetin and kaempferol, which often occur as a complex conjugated via glycosilation and acylation of the aglycone [7]. Frequently, these compounds occur in acylated forms with hydroxycinnamic acids; among them, the most abundant are *p*-coumaric acid, caffeic acid, ferulic acid, and sinapic acids. These complex compositions are influenced by many factors, e.g., cultivar, climate, postharvest treatments, and agricultural and environmental variables [8–11].

Belonging to the Brassicaceae family, *Brassica juncea* L. is an amphiploid species, mainly grown as a food crop but is also used for medicinal purposes. It is one of the richest sources of iron, vitamin A, and vitamin C but also contains potassium, calcium, thiamine, riboflavin, and β -carotene. It has antiseptic, diuretic, emetic, and rubefacient properties. It has been reported to contain antioxidants like flavonoids, carotenes, lutein, indoles, and zeaxanthin [12].

The metabolite profiling of *Brassica juncea* L. has up until now been carried out using high- or ultra-high-performance liquid chromatography (HPLC, UHPLC) coupled with photodiode array (PDA) and/or MS detection [13–18]. However, due to its complexity, related to the simultaneous presence of isobaric molecules, a single separation system *viz.* one-dimensional LC (1D-LC) hampers a full profiling of such complex samples, thus negatively affecting quantification data [14–16]. An alternative expedient for overcoming such an issue could be the use of advanced analytical tools, e.g., comprehensive two-dimensional LC (LC \times LC). The latter, which comprises two orthogonal separation mechanisms, can provide higher resolving power, which is the peak capacity (n_C) multiplicative of the peak capacity values in both dimensions [19–32].

The likelihood of achieving “orthogonal” separation mechanisms in LC \times LC separations is quite high considering the hydrophobicity, polarity, size and charge; however, some technical difficulties can arise as a result of the chosen coupling. As an example, a combination of normal phase (NP) and reversed phase (RP) may lead to the precipitation of buffers or salts due to the mobile phase immiscibility [26,27]. On the other hand, when dealing with RP-LC \times RP-LC separations, no solvent compatibility issues are usually observed. The main issue for such a set-up, using a conventional “full in fraction” in the second dimension (2D) gradient, is the limited orthogonality due the similarity of the stationary phases employed. In fact, the analytes tend to align themselves along the diagonal line in the 2D contour plot. To ameliorate such an issue, some expedients (tailored gradient programs) have been exploited in recent years [19–21,25,30–32]. A first type of gradient is called a “segmented gradient,” where at least two different gradient segments are employed throughout the whole RP-LC \times RP-LC run. As a result, a remarkable bandwidth suppression effect is achieved and the likelihood of the “wrap-around” phenomena is toned down [19,21,22]. A second type of gradient, a parallel gradient mode, involves a single 2D gradient run matching the 1D one. In this case, a longer 2D elution time can be used since a post-gradient equilibration is not necessary [19,21]. Also, the use of “shift gradients” for the 2D run has been proposed with the aim to adopt a (changing) narrower gradient program for the entire RP-LC \times RP-LC analysis time. This approach turned out to be a very effective one in various natural product and food applications [20,25,30–32].

In this contribution, a newly developed RP-LC \times RP-LC system coupled with PDA and MS detection for the untargeted metabolite content of three different cultivars of *Brassica juncea*, namely ISCI 99, ISCI Top and “Broad-leaf,” is reported. Separations were conducted using a combination of a first dimension (1D) microbore cyano column, and a 2D superficially porous RP-Amide column. A novel 2D gradient mode, namely a multi (three-step) segmented-in-fraction gradient, was proposed and successfully demonstrated, leading to an improved expansion of metabolic coverage.

2. Results and Discussion

The analysis of the three different cultivars of *B. juncea* L. was first run using a conventional LC-PDA-MS approach on a C18 column. As illustrated in the following section, a considerable number of compounds overlapped; consequently, an RP-LC×RP-LC system was adopted in order to attain higher separation power, thus providing a thorough overview of the overall metabolites pool, which is beneficial for quantification purposes.

2.1. Elucidation of *Brassica juncea* Cultivars Using RP-LC×RP-LC-PDA-MS

RP-LC×RP-LC separations have proved to be quite effective for the analysis of the metabolite content of food and natural products [19–22,25,30–32]. Before running an RP-LC×RP-LC analysis, a careful optimization of the independent separations must be carried out [26,27,29]. A low mobile phase flow rate is preferred in the ¹D in order to decrease the fraction volume onto the ²D and augment the ¹D sampling rate. Usually, this is achieved by employing a microcolumn in the ¹D; however, since most commercial LC pumps are not capable of delivering a stable and repeatable flow rate, a higher flow rate is commonly employed and split up before entering the ¹D column. A scheme of the RP-LC×RP-LC employed is reported in Figure 1.

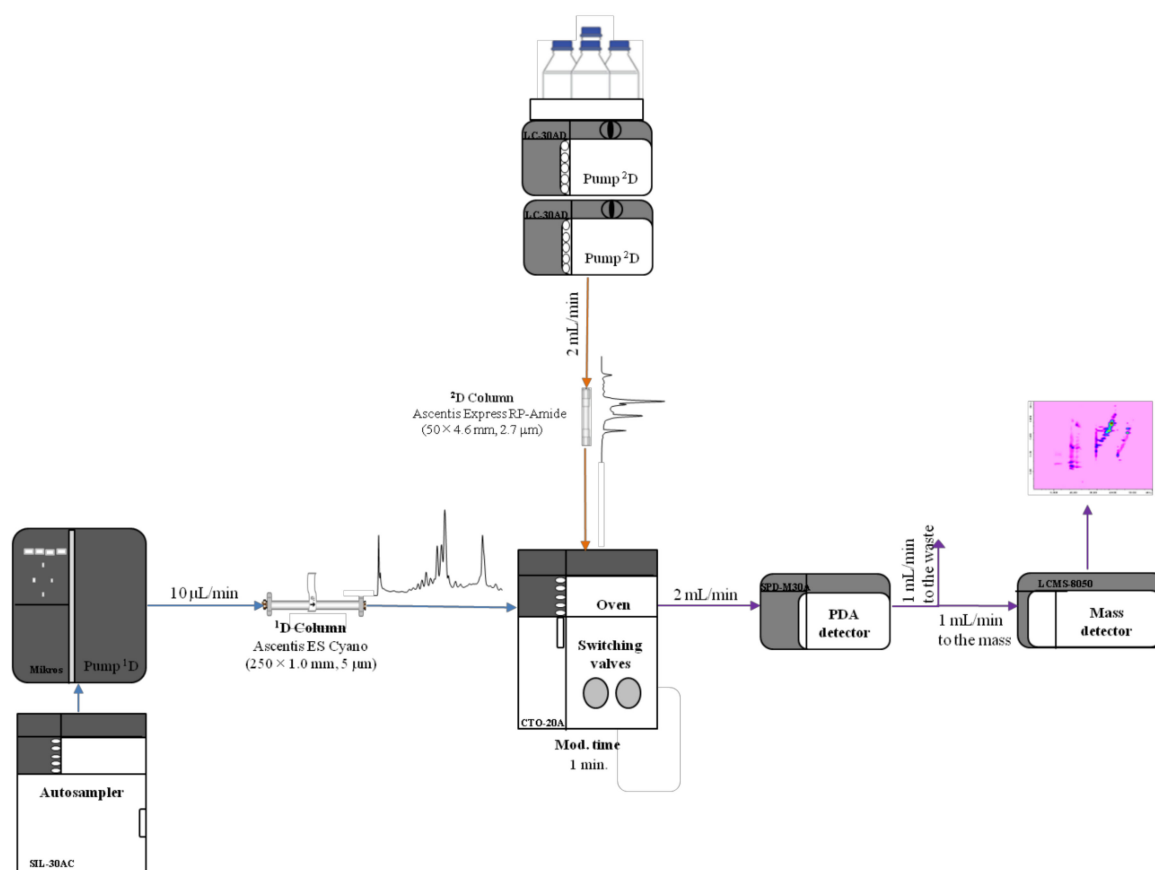
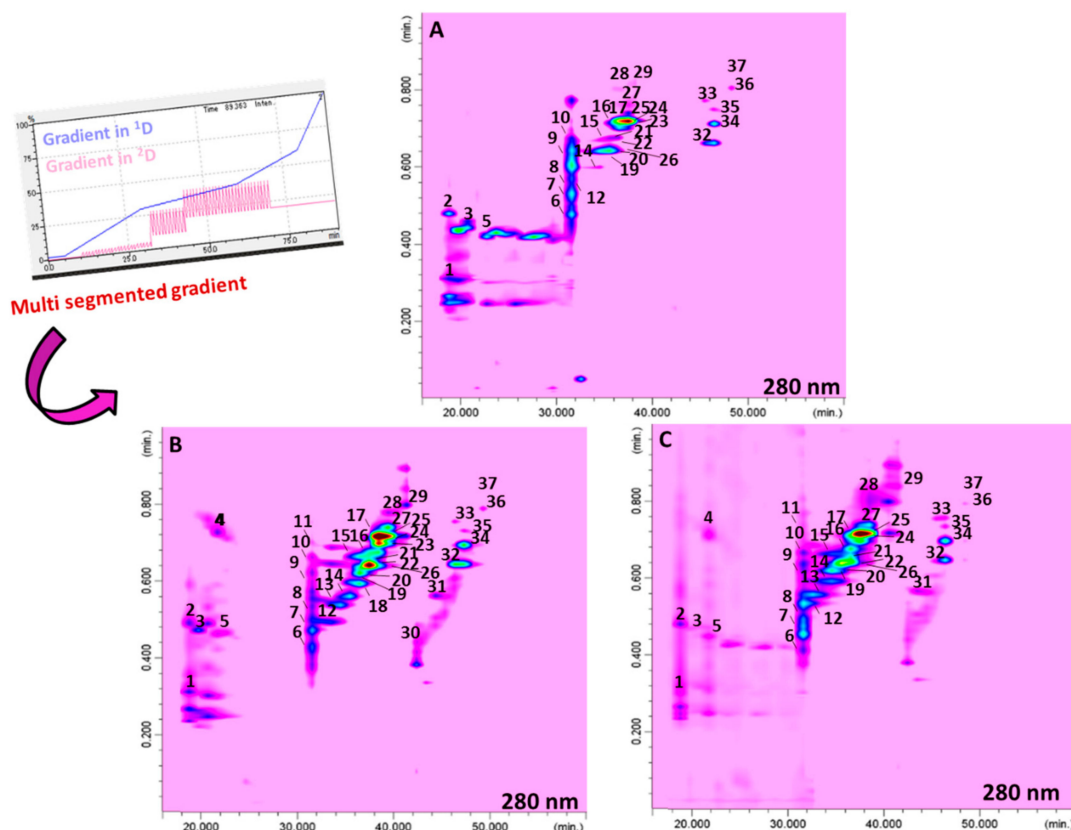


Figure 1. Scheme of the reversed-phase liquid chromatography RP-LC×RP-LC system employed for the investigated work. PDA: Photodiode array.

In this work, a robust and easy-to-use micropump with a completely new direct-drive engineering was advantageously employed, and was capable of delivering micro- to semi-micro flow rates ranging from 1 to 500 µL/min. Repeatability data obtained on four selected peaks are displayed in Table 1. Relative standard deviation (RSD, %) values lower than 0.02 were attained in the case of mean retention times (min), whereas RSD (%) values lower than 1.21 were determined in case of mean areas.

Table 1. Repeatability data calculated from four selected peaks of the RP-LC×RP-LC plots shown in Figure 2. RSD: Relative Standard Deviation. Km: Kaempferol.

No.	Analyte	Mean T _{tr} (min)	RSD (%) n = 3	Mean Area	RSD (%) n = 3
1	Malic acid	19.32	0.02	59664	0.78
2	Km 3-diglucoside-7-glucoside	34.54	0.02	159713	1.21
3	Sinapoyl-feruloyl-triglucoside	42.73	0.01	95465	0.55
4	Disapoylgentiobiose	47.79	0.01	1481389	1.02

**Figure 2.** RP-LC×RP-LC contour plots of the system employed for ISCI Top (A), “Broad-leaf” (B), and ISCI 99 (C).

With regard to the ²D, a fast separation is commonly employed in order to increase the ¹D sampling to lower the risk of incurring wrap-around phenomena. Consequently, a microcyano column was chosen in the ¹D, whereas a 4.6-mm I.D. partially porous RP-Amide column was employed in the ²D and operated at 2 mL min⁻¹. For fraction transfer, two high-speed, six-port, two-position switching valves equipped with two 10 µL sampling loops were chosen.

In this context, the optimization of the gradient programs, especially for the ²D, is also necessary for an adequate separation and is mainly related to the chemical properties of the solutes. Late eluting compounds that are retained more in the ²D require a greater gradient steepness in order not to incur wrap-around effects. In the case of closely related compounds, e.g., early-eluting compounds, which are subjected to co-elutions, a lower gradient of steepness is preferable in order to permit stronger retention.

Following this strategy, a newly developed RP-LC×RP-LC system was investigated. In particular, a multi segmented-in-fraction gradient approach was employed, as illustrated in Figure 2. In particular, three different full-in-fraction gradients were considered for the ²D analysis. The first gradient was from 10 to 32 min, where %B ranged from 3% to 8% (Δ%B: 5) for the analysis of early eluting organic acids; in the second gradient step (from 32 to 43 min), %B ranged from 10% to 44% (Δ%B: 34) for the analysis of (acetylated) tri- and tetrasaccharides, whereas in the last one (from 43 to 60 min), %B ranged

from 20% to 60% ($\Delta\%B$: 40) for the analysis of late eluting (acetylated) mono- and disaccharides. The modulation time of the switching valves was 1.00 min.

Figure 2 shows the contour plots for the RP-LC \times RP-LC analysis of the three cultivars of *Brassica juncea*, where a total of 37, 34, and 31 metabolites were positively separated using the optimized multi segmented-in-fraction gradient approach.

Concerning the performance of the developed RP-LC \times RP-LC system, Table 2 reports the values attained for both peak capacity and orthogonality [33]. The highest theoretical peak capacity values, which are multiplicative of the peak capacity of the two single dimensions [34], were attained for the cultivar ISCI Top (1734), whereas the lowest was obtained for the cultivar ISCI 99 (932). The orthogonality values ranged from 62% to 69% for ISCI Top and “Broad leaf”, respectively [33]. The corrected peak capacity values, which considered, both undersampling [35] and orthogonality values, were 639, 404, and 502 for ISCI Top, ISCI 99, and “Broad leaf”, respectively. Considering the similarity of the two separation systems employed in both dimensions, such values can be considered quite remarkable and are in agreement with previously published findings on similar set-ups exploited for polyphenolic characterization in licorice (695 in Wong et al. [30]) and pistachio (461–633 in Arena et al. [31]) samples.

Table 2. Peak capacity and orthogonality values for the RP-LC \times RP-LC analysis of the three *Brassica juncea* extracts.

Parameter	ISCI Top	ISCI 99	“Broad Leaf”
1D peak capacity, 1n_C	51	34	46
2D peak capacity, 2n_C	34	28	29
Theoretical peak capacity, $^{2D}n_C$	1734	952	1334
Effective peak capacity, $^{2D}n_C$	926	652	772
Orthogonality, A_0	69%	62%	65%
Corrected peak capacity, $^{2D}n_{C,corr}$	639	404	502

As an example, the benefits associated with the employment of the developed RP-LC \times RP-LC with the multi segmented-in-fraction gradient program over the conventional RP-LC separation are highlighted in Figure 3.

A selected chromatographic region of the *Brassica* ISCI Top extract (Figure 3A) clearly shows how the 1D-LC did not provide enough peak capacity for unambiguous characterization of the chemical profile of the three occurring metabolites, due to compound overlapping. However, when the RP-LC \times RP-LC analysis was employed, the three different bioactive compounds were conveniently separated and characterized via inspection of the respective MS spectra (Figure 3B). As a result, the better resolution of the RP-LC \times RP-LC separation (with the 2D operated under the multi (three-step) segmented-in-fraction gradient mode) over the conventional 1D-LC led to a greater metabolite expansion in the RP-LC \times RP-LC space, which was essential for improving the reliable identification of compounds with complexity and/or various polarities.

2.2. Semi-Quantitative Determination of the Flavonoid Content of *Brassica juncea* Cultivars

Tentative identification of the *Brassica juncea* extracts, illustrated in Figure 2, was performed based on their PDA, MS, and literature data [1,2,9–11,14–16,36–38]. Among the major classes of compounds identified, organic acids, (acetylated) tri- and tetrasaccharides, and (acetylated) mono- and disaccharides, were recognized (Table 3). Due to the lack of commercial standards, quantification of *Brassica* spp content has so far been carried out after acidic and/or alkaline hydrolysis [36–38]. In this work, a quantification of the native flavonoid composition of the three cultivars of *Brassica juncea* was carried out by RP-LC \times RP-LC system coupled to PDA detection for the first time. Toward such an aim, and considering the unavailability of corresponding standard references, an established approach in the field of food and natural product analysis was followed. Basically, three standards, as representatives

of the distinct chemical classes, i.e., Km 3-*O*-glucoside, Isorhamnetin (Is) 3-*O*-glucoside, and Qn 3-*O*-glucopyranoside, were chosen and calibration curves were prepared, as reported in Section 3.4.5. Results are shown in Table 4, which reports all the standard curves, correlation coefficients (R^2), limits of detection (LoDs) and limits of quantification (LoQs), and relative standard deviations (RSDs) of the peak areas for each standard selected. The five-point calibration curves provided R^2 values ranging from 0.9993 to 0.9997, whereas for LoQ and LoD, values as low as only 30 ppb and 90 ppb, respectively, were found. Finally, RSD values lower than 0.89% were obtained, demonstrating valuable method repeatability.

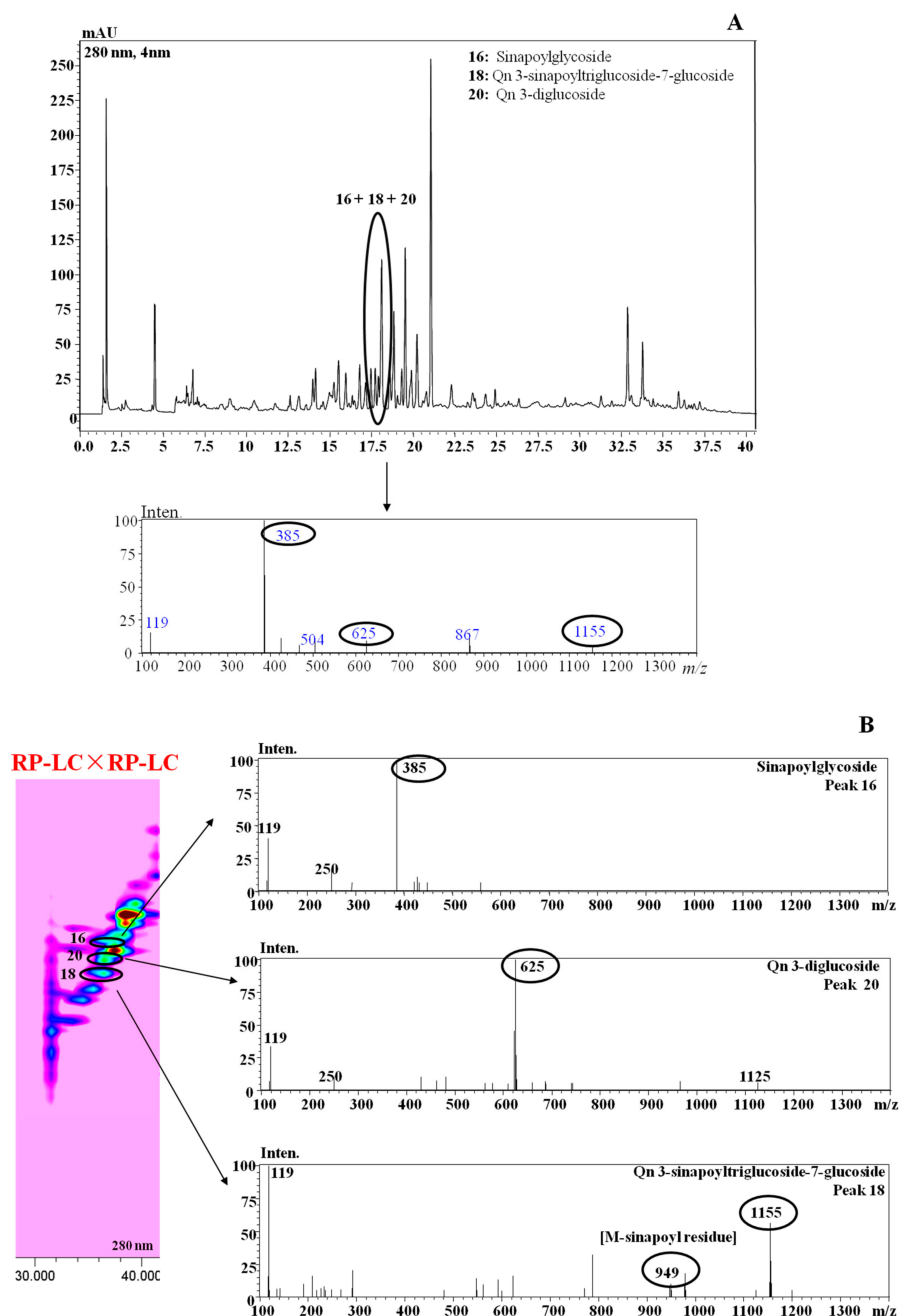


Figure 3. RP-LC (A) vs. RP-LC×RP-LC (B) analysis of metabolites in *B. juncea* cv. ISCI Top. Qn: Quercetin.

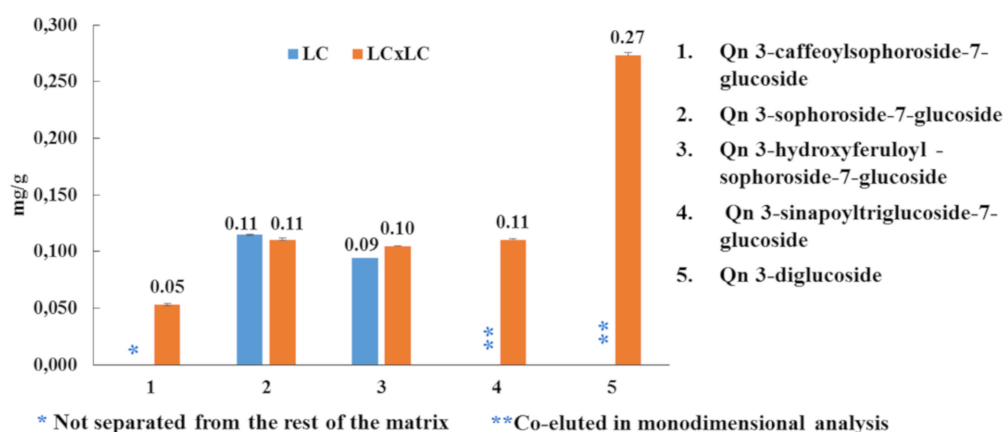
Table 3. Semi-quantitative analysis (mg/kg) of the flavonoid content of *Brassica spp* extracts. Results are expressed as mean \pm S.D. of three replicates.

	Compounds	Molecular Ion [M-H] ⁻	λ_{\max} (nm)	<i>B. juncea</i> cv. ISCI Top	<i>B. juncea</i> cv. "Broad Leaf"	<i>B. juncea</i> cv. ISCI 99
1	Malic acid	133	215; 260	n.q.	n.q.	n.q.
2	Citric acid	191	215; 260	n.q.	n.q.	n.q.
3	Dihydrocaffeic acid 3-O-glucoside	357	250; 323	n.q.	n.q.	n.q.
4	Km 3-dicoumaryl-glucoside	739	202; 257	14.6 \pm 2.1	13.1 \pm 1.5	-
5	1-methoxyspirobrassin	279	198; 259	n.q.	n.q.	n.q.
6	Qn 3-caffeoylsophoroside-7-glucoside	949	250; 336	5.30 \pm 0.1	2.91 \pm 0.1	3.01 \pm 2.2
7	Qn 3-sophoroside-7-glucoside	787	254; 350	11.02 \pm 0.2	23.96 \pm 1.0	1.44 \pm 0.3
8	Sinapoyl-gentiobiose	547	238; 320	n.q.	n.q.	n.q.
9	Rhamnosyl-ellagic acid 1	447	238; 304	n.q.	n.q.	n.q.
10	Rhamnosyl-ellagic acid 2	447	238; 304	n.q.	n.q.	n.q.
11	Feruloylglucose 1	355	243; 328	n.q.	n.q.	-
12	Km 3-O-diglucoside-7-O-glucoside	771	263; 330	33.56 \pm 0.4	27.70 \pm 5.0	3.67 \pm 1.9
13	Km 3-sophoroside-7-glucoside	771	266; 343	45.77 \pm 1.5	80.29 \pm 4.2	-
14	Km 3-caffeoyl-triglucoside-7-glucoside	1095	250; 335	15.97 \pm 0.4	21.34 \pm 1.4	7.39 \pm 0.6
15	Qn 3-hydroxyferuloylsophoroside-7-glucoside	979	250; 337	10.47 \pm 0.1	26.62 \pm 1.1	4.25 \pm 0.9
16	Sinapoylglycoside	385	239; 329	n.q.	n.q.	n.q.
17	Feruloylglucose 2	355	243; 329	n.q.	n.q.	n.q.
18	Qn 3-sinapoyltriglucoside-7-glucoside 1	1155	249; 336	11.05 \pm 0.1	-	-
19	Km 3-hydroxyferuloylsophoroside-7-glucoside	963	264; 334	21.21 \pm 0.5	8.55 \pm 0.3	1.52 \pm 1.1
20	Qn 3-diglucoside	625	255; 345	35.75 \pm 0.3	61.97 \pm 1.9	13.59 \pm 1.5
21	Km 3-O-caffeoyldiglucoside-7-O-glucoside 1	933	249; 335	64.78 \pm 0.4	80.29 \pm 4.2	7.39 \pm 0.6
22	Km 3-sinapoylsophorotrioside-7-glucoside	1139	249; 335	248.54 \pm 8.1	174.38 \pm 1.9	10.88 \pm 0.3
23	Km 3-hydroxyferuloylsophoroside-7-glucoside 2	963	250; 333	27.88 \pm 0.6	-	10.57 \pm 0.3
24	Km 3-sinapoylsophoroside-7-glucoside	977	266; 333	63.36 \pm 0.9	32.92 \pm 1.8	1.65 \pm 0.2
25	Is 3,7-diglucoside	639	264; 336	309.48 \pm 0.4	1321.50 \pm 6.3	130.2 \pm 4.2
26	Km 3-sinapoylsophorotrioside-7-glucoside	1139	241; 335	29.85 \pm 1.7	20.13 \pm 1.4	1.88 \pm 0.3
27	Km 3-feruloylsophoroside-7-glucoside	947	267; 330	28.57 \pm 0.1	19.32 \pm 0.7	6.89 \pm 0.2
28	Km 3-O-coumaroyldiglucoside-7-O-glucoside	917	267; 318	4.56 \pm 0.1	2.22 \pm 0.2	0.41 \pm 0.2
29	Sinapoylferuloyltrigluose	885	262; 325	n.q.	n.q.	n.q.
30	Sinapic acid	223	270; 326	n.q.	-	-
31	Sinapoyhydroxyferuloyldiglycoside	739	273; 329	n.q.	n.q.	-
32	Disapoylgentiobiose	753	240; 330	n.q.	n.q.	n.q.
33	Is glycoside	477	254; 348	20.31 \pm 0.7	45.41 \pm 3.9	6.63 \pm 1.3
34	Sinapoyl-feruloylgentiobiose	723	240; 330	n.q.	n.q.	n.q.
35	Diferuloyldiglucoside	693	245; 329	n.q.	n.q.	n.q.
36	Trisinapoylgentiobiose	959	243; 326	n.q.	n.q.	n.q.
37	Feruoyl-disapoyl-gentiobiose	929	246; 329	n.q.	n.q.	n.q.

Table 4. Quantitative performance of the polyphenolic reference materials used in this study using the RP-LC×RP-LC system coupled to PDA detection.

Reference Material	Standard Curve	R ²	LoD (µg/mL)	LoQ (µg/mL)	Precision (RSD, %)
Qn 3-O-glucopyranoside	$y = 13239x - 9234.3$	0.9993	0.03	0.09	0.80
Is 3-O-glucopyranoside	$y = 1990.7x + 188.37$	0.9997	0.12	0.39	0.72
Km 3-O-glucopyranoside	$y = 4625.7x + 4475.7$	0.9994	0.03	0.12	0.89

Subsequently, all three samples were analyzed and the contents of the target compounds were calculated using commercially-available software, as reported in Table 3. *B. juncea* cv. “Broad-leaf” presented the highest flavonoid content (1962.61 mg/kg), followed by *B. juncea* cv. ISCI Top (1002.03 mg/kg) and *B. juncea* cv. ISCI 99 (211.37 mg/kg). Is 3,7-diglucoside turned out to be the most abundant flavonoid in each cultivar investigated (ISCI Top: 309.48 mg/kg; “Broad-leaf”: 1321.50 mg/kg; ISCI 99: 130.2 mg/kg), followed by Km 3-sinapoylsophorotrioside-7-glucoside (ISCI Top: 284.54 mg/kg; “Broad leaf”: 174.38 mg/kg; ISCI 99: 10.88 mg/kg). Considering the three different flavonoid classes, isorhamnetin derivates were the most abundant flavonoids in the cultivars “Broad-leaf” and ISCI 99 (1366.91 mg/kg vs. 136.83 mg/kg); on the other hand, with regard to the cultivar ISCI Top, kaempferol derivates were detected in the highest amount (598.65 mg/kg). Interestingly, as an example, looking at the quercetin derivates, by using the LC×LC technique, it was possible to quantify all of them, unlike the conventional LC, in which some of the compounds could not be determined due to either co-elutions or matrix interferences (Figure 4).

**Figure 4.** Semi-quantitative results (mg/g) for quercetin derivatives using RP-LC and RP-LC×RP-LC-PDA.

3. Materials and Methods

3.1. Chemical and Reagents

LC-MS-grade water, methanol, acetonitrile, and acetic acid were obtained from Merck Life Science (Merck KGaA, Darmstadt, Germany). Km 3-O-glucoside, Is 3-O-glucoside, and Qn 3-O-glucoside were obtained from Merck Life Science (Merck KGaA, Darmstadt, Germany). Stock solutions of 1000 mg L⁻¹ were prepared for each standard by dissolving 10 mg in 10 mL of methanol.

1D-LC separations were performed on an Ascentis Express C18 column (Merck Life Science, Merck KGaA, Darmstadt, Germany; 150 × 4.6 mm I.D., 2.7 µm dp). LC×LC separations were conducted by using a ¹D Ascentis ES-Cyano (ES-CN) column (Merck Life Science, Merck KGaA, Darmstadt, Germany; 250 × 1.0 mm I.D., 5 µm dp) and a ²D Ascentis Express RP-Amide column (Merck Life Science, Merck KGaA, Darmstadt, Germany; 50 × 4.6 mm I.D., 2.7 µm dp).

3.2. Sample and Sample Preparation

Brassica juncea L. Czern & Coss cv. ISCI 99, ISCI Top, and “Broad-leaf” leaf selections were provided from the *Brassica* collection of Consiglio per la ricerca in agricoltura e l’analisi dell’economia agraria – Centro di Ricerca Cerealicoltura e Colture Industriali (CREA-CI) [39]. Samples were immediately frozen and freeze-dried for storage in glass vacuum desiccators. Lyophilized tissues were finely powdered to 0.5 μm size for analysis. Compound extraction was carried out based on the following protocol [16] with some modifications. The powder of the leaves of the three different *B. juncea* cultivars were weighed into 100 mg samples. The samples were extracted twice with 5 mL of a mixture of methanol:water (60:40, *v/v*) for 30 min in a sonicator and centrifuged at $1000\times g$ for 15 min, followed by filtration of the supernatants through a 0.45- μm nylon filter (Merck Life Science, Merck KGaA, Darmstadt, Germany). The prepared organic extracts were subjected to evaporation in a EZ-2 evaporator and then redissolved in 1 mL of the same solvent extraction mixture of methanol:water (60:40, *v/v*).

3.3. Instrumentation

LC and LC \times LC analyses were performed on a Nexera-e liquid chromatograph (Shimadzu, Kyoto, Japan), consisting of a CBM-20A controller, one LC-Mikros binary pump, two LC-30AD dual-plunger parallel-flow pumps, a DGU-20A₅R degasser, a CTO-20AC column oven, a SIL-30AC autosampler, and an SPD-M30A PDA detector (1.0 μL detector flow cell volume). The two dimensions were connected by means of two high-speed/high-pressure, two-position, six-port switching valves with a micro-electric actuator (model FCV-32 AH, 1.034 bar; Shimadzu, Kyoto, Japan), placed inside the column oven, and equipped with two 10- μL stainless steel loops. The Nexera-e liquid chromatograph was hyphenated to an LCMS-8050 triple quad mass spectrometer through an ESI source (Shimadzu, Kyoto, Japan).

3.4. Analytical Conditions

3.4.1. LC Separations

1D-LC separations were run on the Ascentis Express C18 column. Mobile phases: (A) 0.15% acetic acid in water (pH 3), (B) 0.15% acetic acid in ACN. Gradient: 0 min, 5% B; 5 min, 5% B; 15 min, 10% B; 30 min, 20% B; 60 min, 50% B; 80 min, 100%. Mobile phase flow rate: 1 mL min^{-1} . Column oven: 30 $^{\circ}\text{C}$. Injection volume: 10 μL .

3.4.2. LC \times LC Separations

For ¹D separations, the Ascentis ES-CN column was used. Mobile phases: (A) 0.15% acetic acid in water (pH 3), (B) 0.15% acetic acid in ACN. Gradient: 0 min, 2% B; 5 min, 2% B; 30 min, 30% B; 60 min, 40% B; 80 min, 100% B. Flow rate: 10 $\mu\text{L min}^{-1}$. Column oven: 30 $^{\circ}\text{C}$. Injection volume: 1 μL .

For ²D separations, an RP-Amide column was used. The mobile phases employed were (A) 0.15% acetic acid in water (pH 3), (B) 0.15% acetic acid in ACN. Multi (three-step) segmented-in-fraction gradient conditions: I) 10 to 32 min (cycle: 0.01–0.80 min, 3–8% B; 0.81–1.0 min, 3% B); II) 32 to 43 min (cycle: 0.01–0.80 min, 10–44% B; 0.81–1.0 min, 10% B); III) 43 to 60 min (cycle: 0.01–0.80 min, 20–60% B; 0.81–1.0 min, 20% B). Flow rate: 2 mL min^{-1} , modulation time of the switching valves: 1.00 min, loop internal volume: 10 μL , and column oven: 30 $^{\circ}\text{C}$.

3.4.3. Detection Conditions

PDA range: 200–450 nm; sampling rate: 12.5 Hz (1D-LC analyses), 40 Hz (LC \times LC analyses); time constant: 0.08 sec (1D-LC analyses), 0.025 sec (LC \times LC analyses).

Interface: ESI-MS in negative ionization mode. Mass spectral range in full scan mode: *m/z* 100–1200; event time: 0.5 (1D-LC analyses), 0.2 sec (LC \times LC analyses); nebulizing gas (N_2) flow: 3 L min^{-1} ; drying gas (N_2) flow: 15 L min^{-1} ; heating gas flow (air): 10 L min^{-1} same; heat block

temperature: 400 °C; desolvation line (DL) temperature: 250 °C; interface temperature: 300 °C; interface voltage 3.50 kV; detector voltage: 1.80 kV.

3.4.4. Data Handling

The LC × LC-LCMS-8050 system and the switching valves were controlled using the Shimadzu Labsolution software (ver. 5.93) (Kyoto, Japan). LC×LC-Assist software (ver. 2.00) (Shimadzu, Kyoto, Japan) was used for setting up the multi (three-step) segmented-in-fraction gradient analyses. The LC × LC data were visualized and elaborated into two and three dimensions using Chromsquare ver. 2.3 software (Shimadzu, Kyoto, Japan).

3.4.5. Construction of Calibration Curves

For flavonoid determination, due to the lack of commercial standards, Km 3-O-glucoside, Is 3-O-glucoside, and Qn 3-O-glucopyranoside, as representatives of the distinct chemical classes under evaluation, were selected. Standard calibration curves were prepared in the concentration range 0.1–100 mg L⁻¹ with five different concentration levels, run in triplicate. The amount of the compound was finally expressed in mg kg⁻¹ of extract.

4. Conclusions

In this paper, the benefits associated with the use of a multi (three-step) segmented-in-fraction gradient in the RP-LC×RP-LC-PDA-MS analysis of three *Brassica juncea* cultivars are demonstrated. The coupling of a microcyano and an RP-Amide columns, in the first and second dimension, respectively, provided a characteristic metabolite pattern of the extracts, leading to the identification of 37 bioactives of different chemical nature, i.e., organic acids, (acetylated) tri- and tetrasaccharides, and (acetylated) mono- and disaccharides. Interestingly, the employment of a micro LC pump in the first dimension of the RP-LC×RP-LC-PDA-MS systems allowed for high repeatability and stable retention times and areas. The investigated approach can be advantageously employed for RP-LC×RP-LC metabolic analyses of other complex plant derived extracts.

Author Contributions: Conceptualization, F.C. and P.D.; methodology, K.A.; software, L.M.; validation, F.C., L.M.; investigation, K.A.; resources, L.M.; data curation, F.C., K.A., and P.D.; writing—original draft preparation, K.A.; writing—review and Editing, F.C. and L.D.; visualization, K.A.; supervision, F.C. and P.D.; project Administration, L.M. All authors have read and agree to the published version of the manuscript.

Funding: This research was funded by the Italian Ministry of Research under the Research Project of National Interest 2015 (PRIN 2015): Securing and ensuring sustainable use of agriculture waste, co- and by-products: an integrated analytical approach combining mass spectrometry with health effect-based biosensing, supported by the Italian Ministry of University and Scientific Research, grant number [2015FFY97L].

Acknowledgments: The authors are thankful to Shimadzu and Merck Life Science Corporations for the continuous support.

Conflicts of Interest: The authors declare no conflict of interest.

References

1. Cartea, M.E.; Marta, F.; Soengas, P.; Velasco, P. Phenolic Compounds in *Brassica* Vegetables. *Molecules* **2011**, *6*, 251–280.
2. Podsedek, A. Natural antioxidants and antioxidant capacity of *Brassica* vegetables: A review. *LWT Food Sci. Technol.* **2007**, *40*, 1–11.
3. Kurilich, A.C.; Tsau, G.J.; Brown, A.; Howard, L.; Klein, B.P.; Jeffery, E.H.; Kushad, M.; Wallig, M.A.; Juvik, J.A. Carotene, tocopherol, and ascorbate contents in subspecies of *Brassica oleracea*. *J. Agric. Food Chem.* **1999**, *47*, 1576–1781.
4. Nilsson, J.; Olsson, K.; Engqvist, G.; Ekvall, J.; Olsson, M.; Nyman, M.; Åkesson, B. Variation in the content of glucosinolates, hydroxycinnamic acids, carotenoids, total antioxidant capacity and low-molecular-weight carbohydrates in *Brassica* vegetables. *J. Sci. Food Agric.* **2006**, *86*, 528–538.

5. Beecher, C.W. Cancer preventive properties of varieties of *Brassica oleracea*: A review. *Am. J. Clin. Nutr.* **1994**, *59*, 1166–1170.
6. Kroon, P.; Williamson, G. Polyphenols: dietary components with established benefits to health? *J. Sci. Food Agric.* **2005**, *85*, 1239–1240.
7. Andersen, Ø.M.; Jordheim, M. The Anthocyanins. In *Flavonoids, Chemistry, Biochemistry and Application*; Andersen, Ø.M., Markham, K.R., Eds.; Taylor & Francis Group: Boca Raton, FL, USA, 2006.
8. Winkel-Shirley, B. Biosynthesis of flavonoids and effects of stress. *Curr. Opin. Plant. Biol.* **2002**, *5*, 218–223.
9. Hagen, S.F.; Borge, G.I.A.; Solhaug, K.A.; Bengtsson, G.B. Effect of cold storage and harvest date on bioactive compounds in curly kale (*Brassica oleracea* L. var. *acephala*). *Postharvest Biol. Technol.* **2009**, *51*, 36–42.
10. Zietz, M.; Weckmuller, A.; Schmidt, S.; Rohn, S.; Schreiner, M.; Krumbein, A.; Kroh, L.W. Genotypic and climatic influence on the antioxidant activity of flavonoids in kale (*Brassica oleracea* var. *sabellica*). *J. Agric. Food Chem.* **2010**, *58*, 2123–2130.
11. Schmidt, S.; Zietz, M.; Schreiner, M.; Rohn, S.; Kroh, L.W.; Krumbein, A. Genotypic and climatic influences on the concentration and composition of flavonoids in kale (*Brassica oleracea* var. *sabellica*). *Food Chem.* **2010**, *119*, 1293–1299.
12. Shekhawat, K.; Rathore, S.S.; Premi, O.P.; Kandpal, B.K.; Chauhan, J.S. Advances in agronomic management of Indian mustard (*Brassica juncea* (L.) Czernj. Cosson): An overview. *Int. J. Agron.* **2012**, 408284. [[CrossRef](#)]
13. Thiyam-Holländer, U.; Aladedunye, F.; Logan, A.; Yang, H.; Diehl, B.W.K. Identification and quantification of canolol and related sinapate precursors in Indian mustard oils and Canadian mustard products. *Eur. J. Lipid Sci. Technol.* **2014**, *116*, 1664–1674.
14. Harbaum, B.; Hubbermann, E.M.; Zhu, Z.; Schwarz, K. Impact of Fermentation on Phenolic Compounds in Leaves of Pak Choi (*Brassica campestris* L. ssp. *chinensis* var. *communis*) and Chinese Leaf Mustard (*Brassica juncea* Coss). *J. Agric. Food Chem.* **2008**, *56*, 148–157.
15. Lin, L.-Z.; Sun, J.; Chen, P.; Harnly, J. UHPLC-PDA-ESI/HRMS/MSn Analysis of Anthocyanins, Flavonol Glycosides, and Hydroxycinnamic Acid Derivatives in Red Mustard Greens (*Brassica juncea* Coss Variety). *J. Agric. Food Chem.* **2011**, *59*, 12059–12072.
16. Sun, J.; Xiao, Z.; Lin, L.; Lester, G.E.; Wang, Q.; Harnly, J.M.; Chen, P. Profiling Polyphenols in Five *Brassica* Species Microgreens by UHPLC-PDA-ESI/HRMSⁿ. *J. Agric. Food Chem.* **2013**, *61*, 10960–10970.
17. Oh, S.; Tsukamoto, C.; Kim, K.; Choi, M. Investigation of glucosinolates, and the antioxidant activity of Dolsan leaf mustard kimchi extract using HPLC and LC-PDA-MS/MS. *J. Food Biochem.* **2017**, *41*, 12366.
18. Khattab, R.; Eskin, M.; Aliani, M.; Thiyam, U. Determination of Sinapic Acid Derivatives in Canola Extracts Using High-Performance Liquid Chromatography. *J. Am. Oil Chem. Soc.* **2010**, *87*, 147–155.
19. Jandera, P.; Hájek, T.; Česla, P. Effects of the gradient profile, sample volume and solvent on the separation in very fast gradients, with special attention to the second-dimension gradient in comprehensive two-dimensional liquid chromatography. *J. Chromatogr. A* **2011**, *1218*, 1995–2006.
20. Li, D.; Schmitz, O.J. Use of shift gradient in the second dimension to improve the separation space in comprehensive two-dimensional liquid chromatography. *Anal. Bioanal. Chem.* **2013**, *405*, 6511–6517.
21. Leme, G.M.; Cacciola, F.; Donato, P.; Cavalheiro, A.; Dugo, P.; Mondello, L.; Continuous, vs. segmented second-dimension system gradients for comprehensive two-dimensional liquid chromatography of sugarcane (*Saccharum* spp.). *Anal. Bioanal. Chem.* **2014**, *406*, 4315–4324.
22. Tomasini, D.; Cacciola, F.; Rigano, F.; Sciarrone, D.; Donato, P.; Beccaria, M.; Caramão, E.B.; Dugo, P.; Mondello, L. Complementary analytical liquid chromatography methods for the characterization of aqueous phase from pyrolysis of lignocellulosic biomasses. *Anal. Chem.* **2014**, *86*, 11255–11262.
23. Willemse, C.; Stander, M.A.; Vestner, J.; Tredoux, A.G.J.; De Villiers, A. Comprehensive Two-Dimensional Hydrophilic Interaction Chromatography (HILIC) × Reversed-Phase Liquid Chromatography coupled to High-Resolution Mass Spectrometry (RP-LC-UV-MS) Analysis of Anthocyanins and Derived Pigments in Red Wine. *Anal. Chem.* **2015**, *87*, 12006–12015.
24. Montero, L.; Ibáñez, E.; Russo, M.; Rastrelli, L.; Cifuentes, A.; Herrero, M. Anti-proliferative activity and chemical characterization by comprehensive two-dimensional liquid chromatography coupled to mass spectrometry of phlorotannins from the brown macroalga *Sargassum muticum* collected on North-Atlantic coasts. *J. Chromatogr. A* **2016**, *1428*, 115–125.

25. Donato, P.; Rigano, F.; Cacciola, F.; Schure, M.; Farnetti, S.; Russo, M.; Dugo, P.; Mondello, L. Comprehensive two-dimensional liquid chromatography-tandem mass spectrometry for the simultaneous determination of wine polyphenols and target contaminants. *J. Chromatogr. A* **2016**, *1458*, 54–62.
26. Cacciola, F.; Donato, P.; Sciarrone, D.; Dugo, P.; Mondello, L. Comprehensive liquid chromatography and other liquid-based comprehensive techniques coupled to mass spectrometry in food analysis. *Anal. Chem.* **2017**, *89*, 414–429.
27. Cacciola, F.; Dugo, P.; Mondello, L. Multidimensional liquid chromatography in food analysis. *TRAC Trend Anal. Chem.* **2017**, *96*, 116–123.
28. Sommella, E.; Ismail, O.H.; Pagano, F.; Pepe, G.; Ostacolo, C.; Mazzocanti, G.; Russo, M.; Novellino, E.; Gasparrini, F.; Campiglia, P. Development of an improved online comprehensive hydrophilic interaction chromatography × reversed-phase ultra-high-pressure liquid chromatography platform for complex multiclass polyphenolic sample analysis. *J. Sep. Sci.* **2017**, *40*, 2188–2197.
29. Pirok, B.W.J.; Gargano, A.F.G.; Schoenmakers, P.J. Optimizing separations in online comprehensive two-dimensional liquid chromatography. *J. Sep. Sci.* **2018**, *41*, 68–98.
30. Wong, Y.F.; Cacciola, F.; Fermas, S.; Riga, S.; James, D.; Manzin, V.; Bonnet, B.; Marriott, P.J.; Dugo, P.; Mondello, L. Untargeted profiling of *Glycyrrhiza glabra* extract with comprehensive two-dimensional liquid chromatography-mass spectrometry using multi-segmented shift gradients in the second dimension: Expanding the metabolic coverage. *Electrophoresis* **2018**, *39*, 1993–2000.
31. Arena, K.; Cacciola, F.; Mangraviti, D.; Zoccali, M.; Rigano, F.; Marino, N.; Dugo, P.; Mondello, L. Determination of the polyphenolic fraction of *Pistacia vera* L. kernel extracts by comprehensive two-dimensional liquid chromatography coupled to mass spectrometry detection. *Anal. Bioanal. Chem.* **2019**, *411*, 4819–4829.
32. Russo, M.; Cacciola, F.; Arena, K.; Mangraviti, D.; de Gara, L.; Dugo, P.; Mondello, L. Characterization of the polyphenolic fraction of pomegranate samples by comprehensive two-dimensional liquid chromatography coupled to mass spectrometry detection. *Nat. Prod. Res.* **2019**. [[CrossRef](#)]
33. Camenzuli, M.; Schoenmakers, P.J. A new measure of orthogonality for multi-dimensional chromatography. *Anal. Chim. Acta* **2014**, *838*, 93–101.
34. Neue, U.D. Theory of peak capacity in gradient elution. *J. Chromatogr. A* **2005**, *1079*, 153–161.
35. Gu, H.; Huang, Y.; Carr, P.W. Peak Capacity Optimization in Comprehensive Two Dimensional Liquid Chromatography: A Practical Approach. *J. Chromatogr. A* **2011**, *1218*, 64–73.
36. Harbaum, B.; Hubbermann, E.M.; Wolff, C.; Herges, R.; Zhu, Z.; Schwartz, K. Identification of Flavonoids and Hydroxycinnamic Acids in Pak Choi Varieties (*Brassica campestris* L. ssp. *chinensis* var. *communis*) by HPLC-ESI-MSⁿ and NMR and Their Quantification by HPLC-DAD. *J. Agric. Food Chem.* **2007**, *55*, 8251–8260.
37. Olsen, H.; Aaby, K.; Borge, G.I.A. Characterization and Quantification of Flavonoids and Hydroxycinnamic Acids in Curly Kale (*Brassica oleracea* L. Convar. *acephala* Var. *sabellica*) by HPLC-DAD-ESI-MSⁿ. *J. Agric. Food Chem.* **2009**, *57*, 2816–2825.
38. Olsen, H.; Aaby, K.; Borge, G.I.A. Characterization, Quantification, and Yearly Variation of the Naturally Occurring Polyphenols in a Common Red Variety of Curly Kale (*Brassica oleracea* L. convar. *Acephala* var. *sabellica* cv. 'Redbor'). *J. Agric. Food Chem.* **2010**, *58*, 11346–11354.
39. Lazzeri, L.; Malaguti, L.; Bagatta, M.; D'Avino, L.; Ugolini, L.; De Nicola, G.R.; Casadei, N.; Cinti, S.; Matteo, R.; Iori, R. Characterization of the main glucosinolate content and fatty acid composition in non-food Brassicaceae seeds. *Acta Hort.* **2003**, *1005*, 331–338.

Sample Availability: Samples of the compounds are not available from the authors.



© 2020 by the authors. Licensee MDPI, Basel, Switzerland. This article is an open access article distributed under the terms and conditions of the Creative Commons Attribution (CC BY) license (<http://creativecommons.org/licenses/by/4.0/>).